Geophysical Research Letters

RESEARCH LETTER
10.1029/2025GL116732

Response of Early Winter Precipitation and Storm Activity in the North Atlantic–European–Mediterranean Region to Indian Ocean SST Variability

M. Reale[1], A. Raganato[2], F. D'Andrea[3], M. Adnan Abid[4,5], A. Hochman[6], N. R. Chowdhury[7,8], S. Salon[1], and F. Kucharski[8]

[1]National Institute of Oceanography and Applied Geophysics—OGS, Trieste, Italy, [2]School of Earth and Atmospheric Sciences, Georgia Institute of Technology, Atlanta, GA, USA, [3]Laboratoire de Météorologie Dynamique, IPSL, ENS, PSL Research University, École Polytechnique, Institute Polytechnique de Paris, Sorbonne Université, CNRS, Paris, France, [4]Department of Physics, Atmospheric, Oceanic and Planetary Physics (AOPP), University of Oxford, Oxford, UK, [5]National Centre for Atmospheric Science (NCAS), Oxford, UK, [6]Fredy and Nadine Herrmann Institute of Earth Sciences, The Hebrew University of Jerusalem (HUJI), Jerusalem, Israel, [7]Department of Mathematics, Informatics and Geosciences, University of Trieste, Trieste, Italy, [8]Earth System Physics, The Abdus Salam International Centre for Theoretical Physics, Trieste, Italy

Abstract We investigate the response of winter precipitation and storm activity in the North Atlantic–European–Mediterranean region (NAEM) to the Indian Ocean Dipole (IOD) from 1979 to 2024. We observe a positive NAO-like pattern over NAEM, which appears in December and shifts eastward through February. IOD further modulates precipitation by inducing changes in total precipitation, event frequency, and wet spell duration. The strength of the observed teleconnection is primarily significant in December. Additionally, we observe a reduction in cyclone activity in December over the East Atlantic and Western Mediterranean. These changes in cyclone track density are primarily driven by variations in the Eady Growth Rate, which are linked to enhanced vertical wind shear associated with a strengthened meridional temperature gradient over the NAEM. The results underscore a significant remote impact of the IOD on early winter hydro-climate variability over the NAEM region, offering a potential value for improving sub-seasonal to seasonal prediction.

Plain Language Summary We investigate how the variability in the Indian Ocean Sea Surface Temperature in autumn, known as the Indian Ocean Dipole (IOD), influences the precipitation regime and storm activity in the North Atlantic, Europe, and Mediterranean regions during the winter season. Our results indicate that IOD variability triggers December shifts in atmospheric pressure over these regions and alters precipitation patterns, influencing the frequency and intensity of precipitation events. The strongest impacts are observed at mid-latitudes, with storm activity decreasing over the Eastern Atlantic and Western Mediterranean. These storm changes are tied to stronger temperature contrasts between the north and south part of the domain, which produce significant changes in the vertical wind shear. Our study further supports the idea that Indian Ocean variability may influence the early winter weather in Europe and the Mediterranean—an important insight for improving sub-seasonal to seasonal forecasts.

Key Points:

- Winter precipitation and storm activity shows mainly in December a long-term significant response to the Indian Ocean Dipole
- Spatial changes in the environmental baroclinicity drive the observed changes in the storm activity in December
- Latitudinal variations of baroclinicity are linked to stronger vertical wind shear driven by an enhanced meridional temperature gradient

Supporting Information:

Supporting Information may be found in the online version of this article.

Correspondence to:

M. Reale,
mreale@ogs.it

Citation:

Reale, M., Raganato, A., D'Andrea, F., Abid, M. A., Hochman, A., Chowdhury, N. R., et al. (2025). Response of early winter precipitation and storm activity in the North Atlantic–European–Mediterranean region to Indian Ocean SST variability. *Geophysical Research Letters*, *52*, e2025GL116732. https://doi.org/10.1029/2025GL116732

Received 1 MAY 2025
Accepted 7 AUG 2025

1. Introduction

Understanding precipitation variability and storm activity in the North Atlantic–European–Mediterranean (hereafter NAEM) region is important due to their profound impacts on water resources, infrastructure, and societal resilience (e.g., Khodayar et al., 2025; Seager et al., 2020). This region experiences significant climatic fluctuations, with extreme precipitation and storm events often leading to windstorms, flooding, economic disruptions, and ecological consequences (Lionello et al., 2006; Little et al., 2023; Neu et al., 2012). Large-scale climate drivers, particularly Sea Surface Temperature (SST) anomalies, shape atmospheric circulation patterns in the North Atlantic and European region through stratospheric and tropospheric pathways (e.g., Brönnimann, 2007; Cagnazzo & Manzini, 2009; Jiménez-Esteve & Domeisen, 2018; Saife et al., 2005, and many others) that may influence precipitation distribution and storm development over NAEM (e.g., Terray & Bador, 2025). Understanding remote tropical SST influences on NAEM storm patterns is, therefore, key for improving sub-seasonal to seasonal precipitation forecasts (Manrique-Suñén et al., 2023; Robertson et al., 2018; White et al., 2022).

Among these drivers, the Indian Ocean has gained increasing attention for its role in modulating mid-latitude climate variability through atmospheric teleconnections (Abid et al., 2020, 2021, 2023; Berkovic & Hochman, 2025; Hochman & Gildor, 2025; Hochman et al., 2024; Raganato et al., 2025). Indian Ocean SST variations can shift large-scale weather patterns, modify jet stream dynamics, and influence the trajectories of the storms, potentially increasing extreme weather events in the NAEM region (Hardiman et al., 2020; Terray & Bador, 2025).

The Indian Ocean Dipole (IOD) is an asymmetric pattern of SST between the western and eastern tropical Indian Ocean (Saji et al., 1999). It typically develops from June to August and peaks from September to November (e.g., Wang et al., 2024). This phenomenon can occur independently or as a response to the El Niño–Southern Oscillation (ENSO; e.g., Ashok et al., 2003; Liu et al., 2014; Yang et al., 2015).

IOD has been shown to promote rainfall and flooding (and corresponding landslides and malaria outbreaks) in East Africa as well as drought in Indonesia and southeastern Australia (Wang et al., 2024 and references therein). Saji and Yamagata (2003) detected the influence of the IOD on temperature and precipitation patterns in Europe, northeast Asia, North and South America, and South Africa. Cai et al. (2011) and Weller and Cai (2013) emphasized the significance of the IOD in influencing precipitation variability in Australia.

Nevertheless, several studies have analyzed the links between Tropical Indian Ocean SST and mid-latitude climate variability (e.g., Bader & Latif, 2005). For example, a linear statistical–dynamic method revealed a significant sensitivity of the North Atlantic Oscillation (NAO) to Indian Ocean SST variability (Baker et al., 2019). Recent studies have shown that the pre-conditioning of the IOD in autumn modulates the heating anomalies in the western-central Indian Ocean in early winter, particularly in December, which induces perturbations to the subtropical jet over South Asia (Abid et al., 2023). These jet fluctuations initiate an upper-level wavenumber-3 pattern that travels across the Pacific and projects in phase onto the North Atlantic Oscillation in the NAEM (Abid et al., 2021, 2023; Joshi et al., 2021). More recently, Raganato et al. (2025) have explored teleconnections driven by the autumn IOD in 1981–2019, both independently and with ENSO, finding that the IOD leads its influence on the North Atlantic-European circulation in early winter through a positive-NAO-like signal, while in late winter, that is, February, the upper-level circulation anomalies are primarily linked to ENSO. This occurs through a positive feedback mechanism involving synoptic transients during early winter. Additionally, positive IOD preconditioning promotes a north-south precipitation dipole over Europe, characterized by increased rainfall in northern Europe and drier conditions in southern regions, particularly Spain and the Mediterranean basin. This pattern is accompanied by above-normal warm temperature anomalies across central and northern Europe, aligning with the positive NAO phase during early winter. These outcomes support the analysis of Hardiman et al. (2020), which have shown that the anomalous positive IOD event in 2019/20 led to a positive NAO, with a northward shift in the jet latitude, a slight increase in its strength, and anomalously high precipitation over the UK and northern Europe.

Here, we investigate the long-term response of the precipitation regime and regional storm activity over the North Atlantic–European–Mediterranean (NAEM) region to Indian Ocean SST variability during the boreal winter for the entire satellite era period (1979–2025). To identify the underlying drivers of these changes, we use the Eady Growth Rate as a diagnostic of environmental baroclinicity, highlighting its role in modulating large-scale atmospheric circulation in December in association with IOD activity. By isolating the effects of the IOD from those of ENSO, we aim to disentangle the physical mechanisms linking Indian Ocean SST anomalies to observed circulation changes and surface impacts across NAEM. Ultimately, this analysis supports the importance of improving the knowledge of tropical–extratropical interactions and their relevance for sub-seasonal to seasonal predictability in the region.

2. Data and Methods

2.1. Data

We used 2D winter (December–February) fields from January 1979 to February 2025 at 0.25° resolution from the European Centre for Medium-Range Weather Forecasts' ERA5 reanalysis (Hersbach et al., 2020, 2023). The research region covers the area between 40°W and 55°E and 20°N–70°N. The variables considered in the analysis are hourly precipitation (in mm), monthly Mean Sea Level Pressure (MSLP, in hPa), surface air and sea surface temperature (in K), zonal and meridional wind speed (in m s^{-1}) and potential temperature (in K) at 500 and

850 hPa. All the fields have been detrended using a least-squares fit, and the monthly anomalies have been considered.

To better characterize the impacts of IOD on precipitation patterns over NAEM, we used a subset of climate extreme indices developed by the Climdex project (https://www.climdex.org/, last accessed 3 February 2025). Specifically, we analyzed monthly total precipitation on wet days (prectot, with wet days defined as those with >1 mm of rain), the number of wet days per month (nwet), the Simple Daily Intensity Index (SDII, calculated as prectot divided by nwet), the number of heavy precipitation days per month (R10mm, days with >10 mm of rain), and the Consecutive Wet Day index (CWD), representing the longest stretch of consecutive wet days per month.

2.2. Quantifying Storm Activity in the North Atlantic-European-Mediterranean Region

Storm activity is quantified using cyclone track density. The domain is divided into 2° grid cells, with each cyclone counted once per cell, regardless of how long it remains there, that is, over 6 hr. This resolution improves track visualization while minimizing noise in higher-resolution data (e.g., Reale et al., 2021).

Cyclones are identified using an objective procedure detailed in Lionello et al. (2002) and Reale and Lionello (2013), applied to ERA5 MSLP fields at a 6-hourly temporal resolution and a 0.25° grid spacing (Hersbach et al., 2020). The method detects minima at time t in the MSLP field by tracing the steepest paths leading to each minimum. Cyclone tracks are then reconstructed by linking the minimum locations across successive time steps (t_1, …, t_n).

This approach yields a list of cyclone tracks with their longitude and latitude positions over time, as well as key system characteristics, including minimum MSLP, Depth, Laplacian, and Size (Reale & Lionello, 2013). The algorithm has been broadly applied in intercomparison studies of cyclone activity in the NAEM region based on single and multi-tracking schemes (Flaounas et al., 2018, 2023; Kotsias et al., 2023; Lionello & Giorgi, 2007; Lionello et al., 2002, 2016, 2019; Neu et al., 2012; Reale & Lionello, 2013; Reale et al., 2021; Ulbrich et al., 2013).

Finally, to detect the factors influencing storm activity, we assessed the environmental baroclinicity by using the Eady Growth Rate (EGR), calculated between 500 and 850 hPa as defined by Hoskins and Valdes (1990):

$$\mathrm{EGR} = \alpha f \, (\partial u/\partial z) \, \mathrm{N}^{-1} \tag{1}$$

With α equal to 0.31 (Lindzen & Farrell, 1980), f the Coriolis parameter (in s^{-1}), $\partial u/\partial z$ vertical wind shear (in s^{-1}), and N the Brunt-Vaisala frequency (in s^{-1}).

2.3. Quantifying the Response of Storm Activity to Variations in the IOD

The impact of the IOD is quantified using a linear regression approach, which relates a standardized monthly index to a physical field, for example, MSLP (Raganato et al., 2025). Specifically, the IOD is defined with the Dipole Mode Index (DMI) as the SST difference between the western (10°N–10°S, 50°E–70°E) and eastern (10°S–0°, 90°E–110°E) Indian Ocean (Saji et al., 1999). To monitor the state of ENSO phases, we used the NINO-3.4 SST index calculated over the region spanning 5°S–5°N and 170°W–120°W (Capotondi et al., 2015; Kug et al., 2009). To understand the sole autumn IOD impact on winter precipitation and storm activity over NAEM, we removed ENSO influences from IOD via the following equation:

$$\mathrm{iod\_RES}(t) = \mathrm{IOD}(t) - b^{*}\mathrm{NINO\text{-}3.4}(t) \tag{2}$$

The coefficient b is determined using least-squares linear regression. In this formulation, iod_RES is uncorrelated with NINO-3.4. Although the IOD develops during the autumn season, both indices are computed for October, when the IOD reaches its peak intensity and also a peak in its relationship with ENSO (Abid et al., 2023; Hochman & Gildor, 2025; Marchant et al., 2007; Raganato et al., 2025). IOD and NINO-3.4 time series are, in fact, strongly correlated (Figure S1 in Supporting Information S1, correlation value = 0.63; statistically significant at $p < 0.05$). At the same time, a correlation value of 0.77 is noted between IOD and iod_RES (Figure S1 in Supporting Information S1), which shows SST variability in the Indian Ocean can also be explained independent

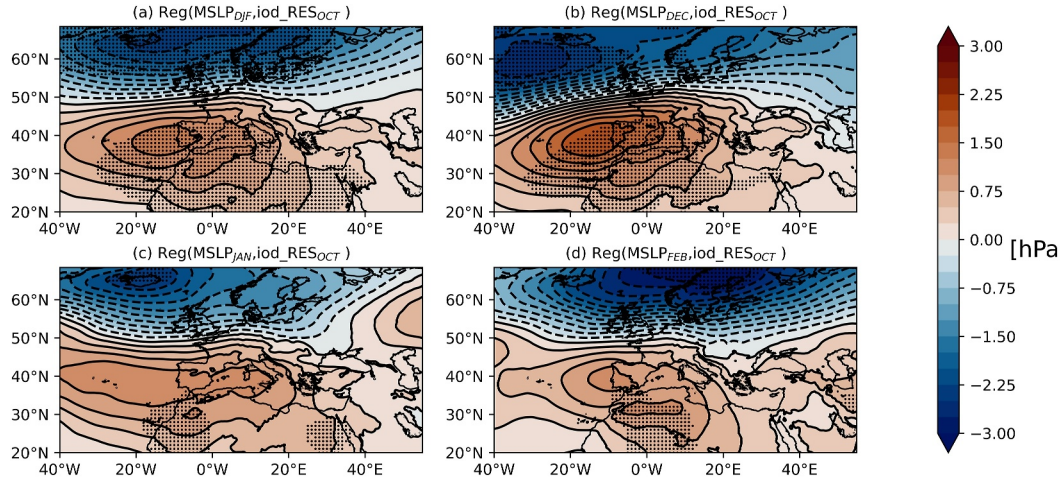

Figure 1. Regression map of DJF (a), December (b), January (c), and February (d) MSLP anomalies (in hPa) onto the corresponding 1979–2024 iod_RES index. Stippling denotes statistical significance of the slope with $p < 0.05$ according to a *t*-test.

of ENSO, consistent with Raganato et al. (2025), where the importance of the preconditioning of the autumn iod_RES for early winter NAO was highlighted, focusing on neutral ENSO conditions.

3. Results

3.1. Linking IOD Variability With Surface Circulation and Precipitation Characteristics

Figure 1 shows the regression maps of the DJF and December, January, and February MSLP against the 1979–2024 iod_RES index. During DJF, in response to the IOD, the NAEM region exhibits a dipole pattern in the MSLP (Hardiman et al., 2020; Figure 1a), with the strongest response, on a monthly scale occurring in December with a robust and statistically significant NAO-like pattern (Figure 1b, Raganato et al., 2025). On the other hand, this dipole in January (c) and February (d) progressively shifts eastward, from the central Atlantic to Scandinavia and the Western Mediterranean by February. At the same time, the strength of the teleconnection significantly weakens, becoming not significant over most of the domain. The negative component in the dipole extends beyond 70°N: however, for sake of consistency with the cyclone tracks climatology (built till 70°N) we limited the visualization of the dipole to the area shown in Figure 1. Abid et al. (2021) attributed the observed dipole structure to a Rossby wave triggered by a convection dipole over the Indian Ocean, which propagates across North America and projects onto the Euro-Atlantic sector. Notably, when the same analysis is applied to NINO-3.4_RES, that is, the ENSO index with IOD effects removed, the MSLP response is opposite in sign but not significant (Figure S2 in Supporting Information S1). The only exception is observed in November (not shown), when ENSO has been shown to influence the Euro-Atlantic circulation via a NAO-like pattern (King et al., 2018).

Figure 2 shows the seasonal DJF and the December–February regression maps for Total precipitation (prectot, a–d), number of wet days (nwet, e–h), Simple Daily Intensity Index (SDII, i–l), number of rainy days with more than 10 mm of rain (R10mm, m–p), and Consecutive Wet Days (CWD, q–t) against the iod_RES index. In DJF (Figure 2a), prectot, nwet, SDII, and CWD mirror the patterns in the MSLP pressure observed in Figure 1a, with December leading the response to the IOD (Figure 2b). This response is again a dipole pattern that initially centers over the North Atlantic and gradually shifts eastward. Increased precipitation, more frequent, intense, and long-lasting rainy events, occur between 50°N–60°N and 40°W–0°W, while the opposite signal prevails over the Atlantic (30°N–40°N) and the Western-Central Mediterranean. Again, as observed before for MSLP, by January and February, the response of the precipitation regime to IOD is weaker and largely insignificant, except in areas such as the UK, Northern Europe, and Scandinavia.

3.2. Linking IOD Variability With Cyclone Activity

Figures 3a–3d presents the DJF and December–February cyclone track density regression maps against the iod_RES index. In DJF, the spatial pattern exhibits some resemblance to the MSLP anomalies observed in

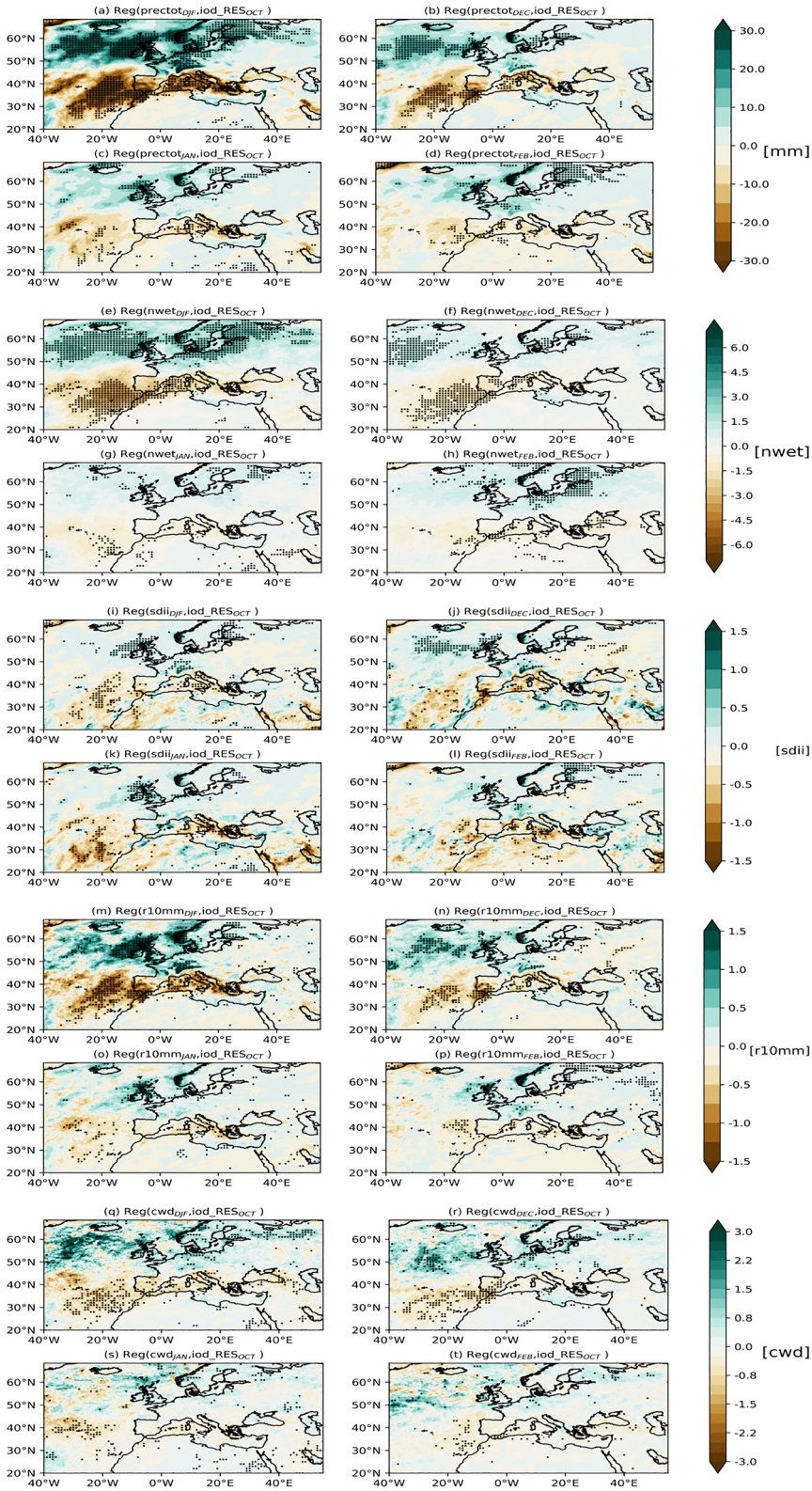

Figure 2. Regression map of prectot (a–d, in mm month^{-1}), nwet (e–h, number of days month^{-1}), SDII (i–l, mm number of wet day for month^{-1}), R10mm (m–p, number of days with precipitation greater than 10 mm month^{-1}) and CWD (q–t, maximum number of consecutive wet days month^{-1}) onto the corresponding 1979–2024 iod_RES in DJF (a, e, i, m, q), December (b, f, j, n, r), January (c, g, k, o, s) and February (d, h, l, p, t). Stippling denotes statistical significance of the slope with $p < 0.05$ according to a *t*-test.

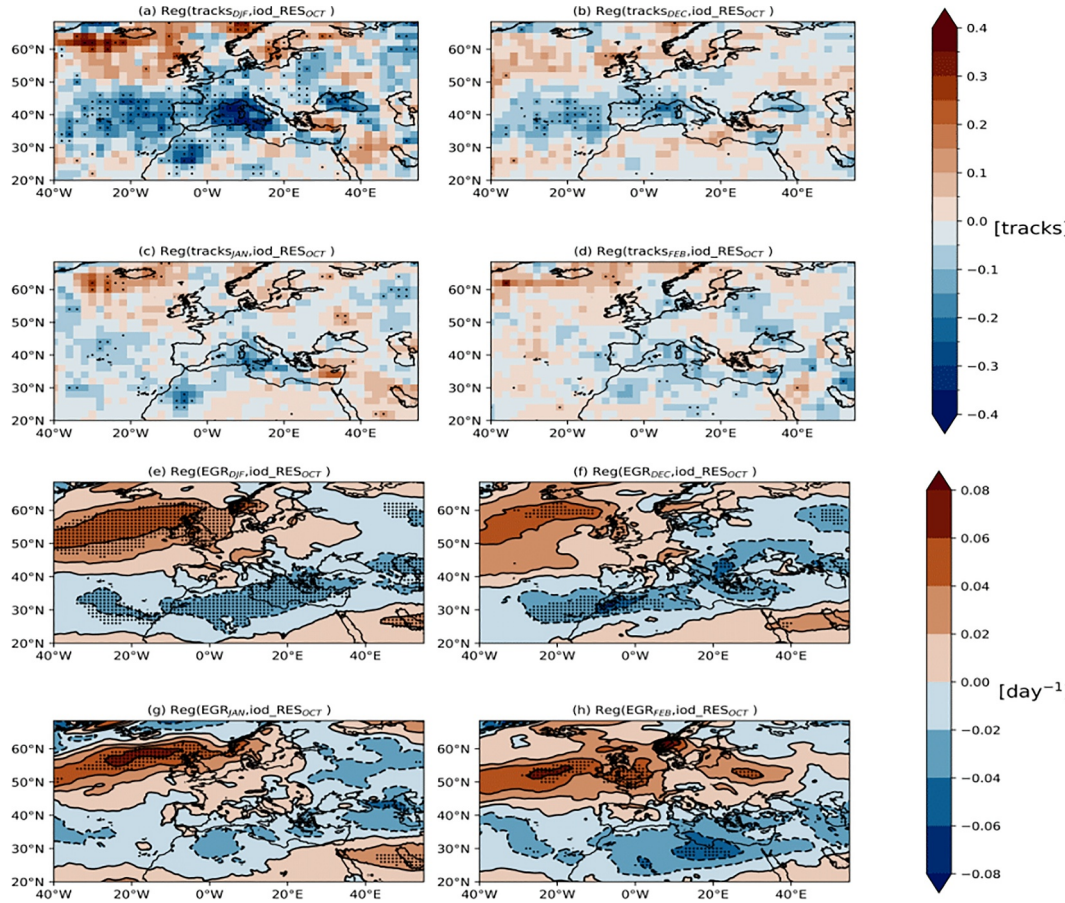

Figure 3. Regression map of density tracks anomalies (number of tracks for 2°; a–d) and EGR between 500 and 850 hPa (in day^{-1}; e–h), in DJF (a, e), December (b, f), January (c, g) and February (d, h) onto the corresponding 1979–2024 iod_RES. Stippling denotes statistical significance of the slope with $p < 0.05$ according to a *t*-test.

Figure 1a and the precipitation changes observed in Figure 2a. A significant decrease in cyclone activity in response to the IOD is observed on a seasonal scale at mid-latitudes (between 30°N and 45°N) over the Eastern Atlantic and Western Mediterranean, whereas an increase is noted between Greenland and Iceland. Again, as observed before for MSLP and precipitation regime, December is the month leading the response to IOD in DJF with a decrease in the density of tracks over most of the Eastern Atlantic and Western Mediterranean (Figure 3b). While this pattern gradually shifts northward toward 70°N and eastward, extending into Scandinavia and the Mediterranean, a weakening of the strength of the response is observed over the domain. Notably, in January, reduced storm activity remains present over part of Western Africa, while an increase is observed around Iceland (Figure 3c).

It is worthwhile to note that the increase in precipitation observed between 50°N–60°N and 40°W–0°W in December (Figure 2b) fits spatially with a modest and not significant increase in the density of tracks (Figure 3b). The explanation for that can be traced back to additional mechanics that can amplify the precipitation associated with cyclones although in presence of limited changes in track density. The analysis of total column vertically-integrated moisture convergence flux (not shown here) has revealed that the precipitation increase is associated with a significantly increased moisture convergence flux between 50°N–60°N and 40°W–0°W. This signal reflects the relationship between cyclonic circulation and moisture transport, where cyclones enhance moisture transport through the low levels of the atmosphere (e.g., Reale & Lionello, 2013; Coll-Hidalgo et al., 2024, and references therein) even in the absence of significant changes in the density of tracks.

Changes in storm activity over the NAEM region, observed in DJF and December, align closely with variations in baroclinicity across much of the domain (Figures 3e and 3f). In DJF and December, the EGR response to the IOD

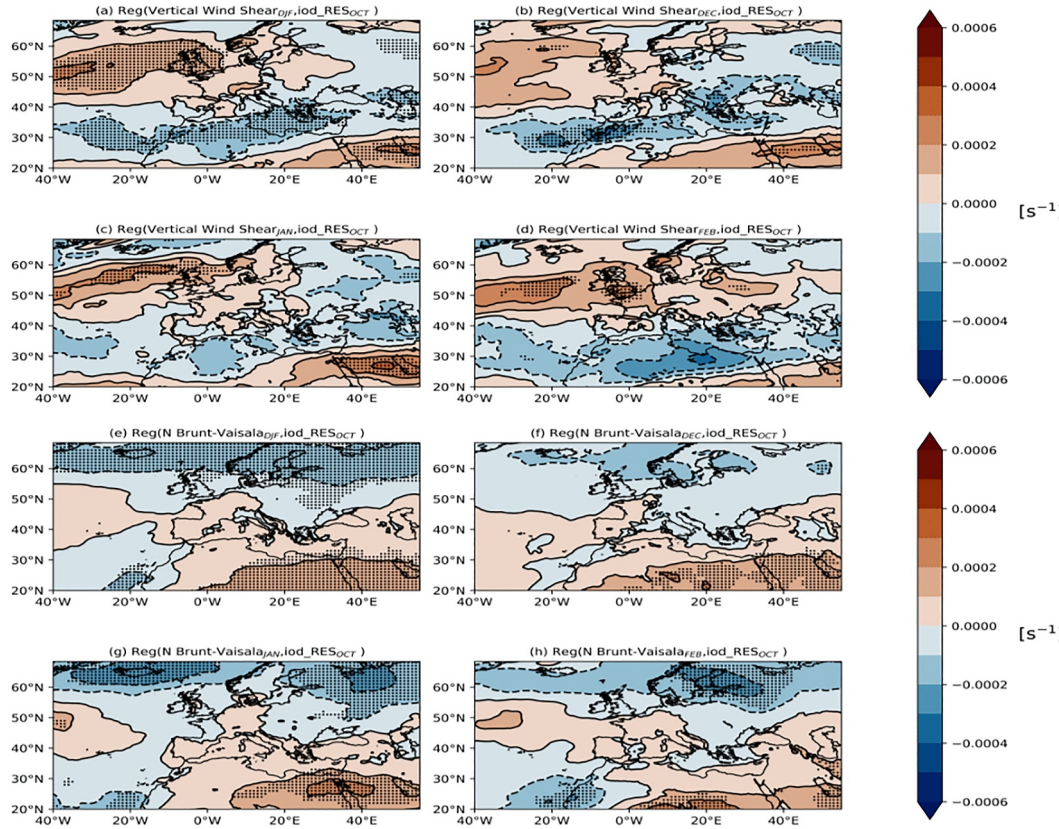

Figure 4. Regression map of vertical wind shear (in s^{-1}; a–d) and vertical stability (in s^{-1}, e–h) in DJF (a, e), December (b, f), January (c, g) and February (d, h) onto the corresponding 1979–2024 iod_RES. Stippling denotes statistical significance of the slope with $p < 0.05$ according to a *t*-test.

mirrors the MSLP and storm track density patterns (Figures 1 and 3), showing a pronounced north–south structure. Notably, it increases over the northern Atlantic (50°N–60°N) while a significant decrease is observed across southern NAEM, the Mediterranean, the Middle East, and the Anatolian Peninsula. Moreover, EGR increases in January close to Iceland.

As shown in Equation 1, changes in the baroclinicity can be driven by changes in the vertical wind shear or vertical stratification measured by N (e.g., D'Andrea et al., 2024). Both factors are shown in Figures 4a–4h. Again, in DJF and December, the increase (or decrease) in EGR corresponds to an increase (or decrease) in vertical wind shear, which is prevalent in relation to the changes in vertical stability. The only exception is the change in EGR observed in January near Iceland, which spatially aligns with the previously noted changes in cyclone activity (Figure 3c) and can be attributed to pronounced variations in vertical stability (Figure 4g).

The changes in EGR and vertical wind shear largely align with the strengthening of the meridional gradient of surface temperature and sea surface temperature in DJF and December, as shown in Figures S3 and S4a–S4d in Supporting Information S1. Specifically, significant warming is observed over most of the Atlantic Ocean and Western and Northern Europe. At the same time, cooling is evident over the northern Atlantic above 50°N and much of the Middle East.

4. Conclusions

This study highlights the significant influence of the Indian Ocean Dipole (IOD) variability on the early winter hydro-climate regime in the North Atlantic–European–Mediterranean region (NAEM; Hardiman et al., 2020; Raganato et al., 2025). Moreover, the IOD here emerges as a key tropical driver of mid-latitude variability, with impacts that extend into the North Atlantic and Mediterranean storm tracks. In fact, the observed north–south dipole in cyclone activity suggests a robust teleconnection pattern in which autumn IOD preconditioning

affects the early winter months, mainly December, where a statistically significant link is noted and linked to baroclinicity and vertical shear shifts, consistent with changes in the meridional temperature gradient.

Our results emphasize the growing importance of understanding tropical-extratropical teleconnections in subseasonal to seasonal forecasts of NAEM (Karpechko et al., 2024; Molteni et al., 2015, and references therein; Molteni & Brookshaw, 2023). As the Indian Ocean emerges as a key modulator of early winter variability over the North Atlantic–European–Mediterranean region, the ability to anticipate its impacts on storm activity and precipitation becomes increasingly relevant for both climate science and decision-making. These findings offer valuable insights for improving the representation of tropical forcing in seasonal forecast systems and may inform efforts to enhance preparedness for weather-related risks in sensitive regions such as the Mediterranean basin. As climate change continues to reshape the background state of both the Indian Ocean and midlatitude circulation, further research is essential to assess the non-stationarity and potential intensification or disruption of the IOD–NAEM link (e.g., Abram et al., 2020; Fereday et al., 2025; Hardiman et al., 2020; Hochman & Gildor, 2025; Sabatani & Gualdi, 2025). Integrating such knowledge into forecasting frameworks holds promise for advancing actionable early warning capabilities across the Euro-Mediterranean sector.

Data Availability Statement

All data used are open and publicly available. ERA5 data are available from the Copernicus Climate Change Service (C3S) Climate Data Store (CDS) (Hersbach et al., 2023).

Acknowledgments
This work has been supported by OGS and CINECA under the High-Performance Computing Training and Research for Earth Sciences (HPC-TRES) program founded by PRACE-Italy national research infrastructure. M. Reale was supported by the National Recovery and Resilience Plan project TeRABIT (Terabit network for Research and Academic Big data in Italy—IR0000022—PNRR Missione 4, Componente 2, Investimento 3.1 CUP I53C21000370006) in the frame of the European Union—NextGenerationEU funding. We acknowledge the CINECA award under the ISCRA initiative and the supercomputing resources and support from ICSC—Centro Nazionale di Ricerca in High Performance Computing, Big Data and Quantum Computing—Spoke 4 Earth and Climate and hosting entity, funded by European Union—NextGenerationEU. M. Adnan Abid was supported by the U.K. Research and Innovation (UKRI) under the U.K. government's Horizon Europe project (ASPECT) Grant [101081460]. The Israel Science Foundation (Grant 978/23), the Ministry of Science, Innovation, and Technology of Israel (Grant 4749), the Federal Ministry of Education and Research (BMBF), Germany, and the Ministry of Innovation Science and Technology of Israel within the GRaCCE project and the Planning and Budgeting Committee of the Israeli Council for Higher Education under the "MedWORLD" Consortium support A.H's contribution.

References

Abid, M. A., Ashfaq, M., Kucharski, F., Evans, K. J., & Almazroui, M. (2020). Tropical Indian Ocean mediates ENSO influence over Central Southwest Asia during the wet season. *Geophysical Research Letters*, *47*(18), e2020GL089308. https://doi.org/10.1029/2020GL089308

Abid, M. A., Kucharski, F., Molteni, F., & Almazroui, M. (2023). Predictability of Indian Ocean precipitation and its North Atlantic teleconnections during early winter. *npj Climate and Atmospheric Science*, *6*(1), 17. https://doi.org/10.1038/s41612-023-00328-z

Abid, M. A., Kucharski, F., Molteni, F., Kang, I.-S., Tompkins, A. M., & Almazroui, M. (2021). Separating the Indian and Pacific Ocean impacts on the Euro-Atlantic response to ENSO and its transition from early to late winter. *Journal of Climate*, *34*(4), 1531–1548. https://doi.org/10.1175/JCLI-D-20-0075.1

Abram, N. J., Wright, N. M., Ellis, B., Dixon, B. C., Wurtzel, J. B., England, M. H., et al. (2020). Coupling of Indo-Pacific climate variability over the last millennium. *Nature*, *579*(7799), 385–392. Epub 2020 Mar 9. Erratum in: Nature. 2022 Feb;602(7896):E20. doi: 10.1038/s41586-021-04318-0. PMID: 32188937. https://doi.org/10.1038/s41586-020-2084-4

Ashok, K., Guan, Z., & Yamagata, T. (2003). A look at the relationship between the ENSO and the Indian Ocean dipole. *Journal of the Meteorological Society of Japan Series II*, *81*(1), 41–56. https://doi.org/10.2151/jmsj.81.41

Bader, J., & Latif, M. (2005). North Atlantic Oscillation response to anomalous Indian Ocean SST in a coupled GCM. *Journal of Climate*, *18*(24), 5382–5389. https://doi.org/10.1175/JCLI3577.1

Baker, H. S., Woollings, T., Forest, C. E., & Allen, M. R. (2019). The linear sensitivity of the North Atlantic oscillation and Eddy driven jet to SSTs. *Journal of Climate*, *32*(19), 6491–6511. https://doi.org/10.1175/JCLI-D-19-0038.1

Berkovic, S., & Hochman, A. (2025). Links between the Indian Ocean dipole and persistent dry spells in the Eastern Mediterranean Winter. https://doi.org/10.2139/ssrn.4999620

Brönnimann, S. (2007). Impact of El Niño–Southern Oscillation on European climate. *Reviews of Geophysics*, *45*, RG3003. https://doi.org/10.1029/2006RG000199

Cagnazzo, C., & Manzini, E. (2009). Impact of stratosphere on the winter troposphere teleconnections between ENSO and the North Atlantic and European Region. *Journal of Climate*, *22*(5), 1223–1238. https://doi.org/10.1175/2008JCLI2549.1

Cai, W., van Rensch, P., Cowan, T., & Hendon, H. H. (2011). Teleconnection pathways of ENSO and the IOD and the mechanisms for impacts on Australian rainfall. *Journal of Climate*, *3910–24*(15), 3923. https://doi.org/10.1175/2011JCLI4129.1

Capotondi, A., Wittenberg, A. T., Newman, M., Di Lorenzo, E., Yu, J. Y., Braconnot, P., et al. (2015). Understanding ENSO diversity. *Bulletin of the American Meteorological Society*, *96*(6), 921–938. https://doi.org/10.1175/BAMS-D-13-00117.1

Coll-Hidalgo, P., Gimeno-Sotelo, L., Fernández-Alvarez, J. C., Nieto, R., & Gimeno, L. (2024). North Atlantic extratropical cyclone tracks and Lagrangian-derived moisture uptake dataset. *Scientific Data*, *11*(1), 1258. https://doi.org/10.1038/s41597-024-04091-5

D'Andrea, F., Duvel, J. P., Rivière, G., Vautard, R., Cassou, C., Cattiaux, J., et al. (2024). Summer deep depressions increase over the Eastern North Atlantic. *Geophysical Research Letters*, *51*(5), e2023GL104435. https://doi.org/10.1029/2023gl104435

Fereday, D. R., Knight, J. R., & Scaife, A. A. (2025). Climate change alters the Indian Ocean Dipole and weakens its North Atlantic teleconnection. *Communications Earth & Environment*, *6*(1), 152. https://doi.org/10.1038/s43247-025-02131-5

Flaounas, E., Aragão, L., Bernini, L., Dafis, S., Doiteau, B., Flocas, H., et al. (2023). A composite approach to produce reference datasets for extratropical cyclone tracks: Application to Mediterranean cyclones. *Weather and Climate Dynamics*, *4*(3), 639–661. https://doi.org/10.5194/wcd-4-639-2023

Flaounas, E., Kelemen, F. D., Wernli, H., Gaertner, M. A., Reale, M., Sanchez-Gomez, E., et al. (2018). Assessment of an ensemble of ocean–atmosphere coupled and uncoupled regional climate models to reproduce the climatology of Mediterranean cyclones. *Climate Dynamics*, *51*(3), 1023–1040. https://doi.org/10.1007/s00382-016-3398-7

Hardiman, S. C., Dunstone, N. J., Scaife, A. A., Smith, D. M., Knight, J. R., Davies, P., et al. (2020). Predictability of European winter 2019/20: Indian Ocean dipole impacts on the NAO. *Atmospheric Science Letters*, *21*(12), e1005. https://doi.org/10.1002/asl.1005

Hersbach, H., Bell, B., Berrisford, P., Biavati, G., Horányi, A., Muñoz Sabater, J., et al. (2023). ERA5 monthly averaged data on single levels from 1940 to present [Dataset]. *Copernicus Climate Change Service (C3S) Climate Data Store (CDS)*. https://doi.org/10.24381/cds.f17050d7

Hersbach, H., Bell, B., Berrisford, P., Hirahara, S., Horányi, A., Muñoz-Sabater, J., et al. (2020). The ERA5 global reanalysis. *Quarterly Journal of the Royal Meteorological Society*, *146*(730), 1999–2049. https://doi.org/10.1002/qj.3803

Hochman, A., & Gildor, H. (2025). Synergistic effects of El Niño–Southern Oscillation and the Indian Ocean Dipole on Middle Eastern subseasonal precipitation variability and predictability. *Quarterly Journal of the Royal Meteorological Society*, *151*(766), e4903. https://doi.org/10.1002/qj.4903

Hochman, A., Shachar, N., & Gildor, H. (2024). Unraveling sub-seasonal precipitation variability in the Middle East via Indian Ocean sea surface temperature. *Scientific Reports*, *14*(1), 2919. https://doi.org/10.1038/s41598-024-53677-x

Hoskins, B. J., & Valdes, P. J. (1990). On the existence of stormtracks. *Journal of the Atmospheric Sciences*, *47*, 1854–1864. https://doi.org/10.1175/1520-0469(1990)047<1854:OTEOST>2.0.CO;2

Jiménez-Esteve, B., & Domeisen, D. I. V. (2018). The tropospheric pathway of the ENSO–North Atlantic teleconnection. *Journal of Climate*, *31*(11), 4563–4584. https://doi.org/10.1175/JCLI-D-17-0716.1

Joshi, M. K., Abid, M. A., & Kucharski, F. (2021). The role of an Indian Ocean heating dipole in the ENSO teleconnection to the North Atlantic European region in early winter during 20th century in reanalysis and CMIP5 simulations. *Journal of Climate*, *34*(3), 1047–1060. https://doi.org/10.1175/JCLI-D-200269.1

Karpechko, A. Y., Vitart, F., Statnaia, I., Alonso Balmaseda, M., Charlton-Perez, A. J., & Polichtchouk, I. (2024). The tropical influence on subseasonal predictability of wintertime stratosphere and stratosphere–troposphere coupling. *Quarterly Journal of the Royal Meteorological Society*, *150*(760), 1357–1374. https://doi.org/10.1002/qj.4649

Khodayar, S., Kushta, J., Catto, J. L., Dafis, S., Davolio, S., Ferrarin, C., et al. (2025). Mediterranean cyclones in a changing climate: A review on their socio-economic impacts. *Reviews of Geophysics*, *63*(2), e2024RG000853. https://doi.org/10.1029/2024rg000853

King, M. P., Herceg-Bulić, I., Kucharski, F., & Keenlyside, N. (2018). Interannual tropical Pacific sea surface temperature anomalies teleconnection to Northern Hemisphere atmosphere in November. *Climate Dynamics*, *50*(5–6), 1881–1899. https://doi.org/10.1007/s00382-017-3727-5

Kotsias, G., Lolis, C. J., Hatzianastassiou, N., Bakas, N., Lionello, P., & Bartzokas, A. (2023). Objective climatology and classification of the Mediterranean cyclones based on the ERA5 data set and the use of the results for the definition of seasons. *Theoretical and Applied Climatology*, *152*(1), 581–597. https://doi.org/10.1007/s00704-023-04374-8

Kug, J.-S., Jin, F.-F., & An, S.-I. (2009). Two types of El Niño events: Cold tongue El Niño and warm pool El Niño. *Journal of Climate*, *22*(6), 1499–1515. https://doi.org/10.1175/2008JCLI2624.1

Lindzen, R. S., & Farrell, B. (1980). A simple approximate result for the maximum growth rate of baroclinic instabilities. *Journal of the Atmospheric Sciences*, *37*(7), 1648–1654. https://doi.org/10.1175/1520-0469(1980)037<1648:asarft>2.0.co;2

Lionello, P., Conte, D., & Reale, M. (2019). The effect of cyclones crossing the Mediterranean region on sea level anomalies on the Mediterranean Sea coast. *Natural Hazards and Earth System Sciences*, *19*(7), 1541–1564. https://doi.org/10.5194/nhess-19-1541-2019

Lionello, P., Dalan, F., & Elvini, E. (2002). Cyclones in the Mediterranean Region: The present and the doubled CO_2 climate scenarios. *Climate Research*, *22*, 147–159. https://doi.org/10.3354/cr022147

Lionello, P., & Giorgi, F. (2007). Winter precipitation and cyclones in the Mediterranean region: Future climate scenarios in a regional simulation. *Advances in Geosciences*, *12*(12), 153–158. https://doi.org/10.5194/adgeo-12-153-2007

Lionello, P., Malanotte-Rizzoli, P., Boscolo, R., Alpert, P., Artale, V., Li, L., et al. (2006). The Mediterranean climate: An overview of the main characteristics and issues. *Developments in Earth and Environmental Sciences*, *4*, 1–26. https://doi.org/10.1016/s1571-9197(06)80003-0

Lionello, P., Trigo, I. F., Gil, V., Liberato, M. L., Nissen, K. M., Pinto, J. G., et al. (2016). Objective climatology of cyclones in the Mediterranean region: A consensus view among methods with different system identification and tracking criteria. *Tellus*, *68*(1), 29391. https://doi.org/10.3402/tellusa.v68.29391

Little, A. S., Priestley, M. D. K., & Catto, J. L. (2023). Future increased risk from extratropical windstorms in northern Europe. *Nature Communications*, *14*(1), 4434. https://doi.org/10.1038/s41467-023-40102-6

Liu, L., Xie, S., Zheng, X., Li, T., Du, Y., Huang, G., & Yu, W. (2014). Indian Ocean variability in the CMIP5 multi-model ensemble: The zonal dipole mode. *Climate Dynamics*, *43*(5–6), 1715–1730. https://doi.org/10.1007/s00382-013-2000-9

Manrique-Suñén, A., Palma, L., Gonzalez-Reviriego, N., Doblas-Reyes, F. J., & Soret, A. (2023). Subseasonal predictions for climate services, a recipe for operational implementation. *Climate Services*, *30*, 100359. https://doi.org/10.1016/j.cliser.2023.100359

Marchant, R., Mumbi, C., Behera, S., & Yamagata, T. (2007). The Indian Ocean dipole the unsung driver of climatic variability in East Africa. *African Journal of Ecology*, *45*(1), 4–16. https://doi.org/10.1111/j.1365-2028.2006.00707.x

Molteni, F., & Brookshaw, A. (2023). Early- and late-winter ENSO teleconnections to the Euro-Atlantic region in state-of-the-art seasonal forecasting systems. *Climate Dynamics*, *61*(5–6), 2673–2692. https://doi.org/10.1007/s00382-023-06698-7

Molteni, F., Stockdale, T. N., & Vitart, F. (2015). Understanding and modelling extra-tropical teleconnections with the Indo-Pacific region during the northern winter. *Climate Dynamics*, *45*(11–12), 3119–3140. https://doi.org/10.1007/s00382-015-2528-y

Neu, U., Akperov, M. G., Bellenbaum, N., Benestad, R., Blender, R., Caballero, R., et al. (2012). IMILAST—A community effort to intercompare extratropical cyclone detection and tracking algorithms: Assessing method-related uncertainties. *Bulletin of the American Meteorological Society*, *94*(4), 529–547. https://doi.org/10.1175/BAMS-D-11-00154.1

Raganato, A., Abid, M. A., & Kucharski, F. (2025). The combined link of the Indian Ocean dipole and ENSO with the North Atlantic–European circulation during early boreal winter in reanalysis and the ECMWF SEAS5 hindcast. *Journal of Climate*, *38*(2), 445–460. https://doi.org/10.1175/JCLI-D-23-0703.1

Reale, M., Cabos Narvaez, W. D., Cavicchia, L., Conte, D., Coppola, E., Flaounas, E., et al. (2021). Future projections of Mediterranean cyclone characteristics using the Med-CORDEX ensemble of coupled regional climate system models. *Climate Dynamics*, *58*(9–10), 1–24. https://doi.org/10.1007/s00382-021-06018-x

Reale, M., & Lionello, P. (2013). Synoptic climatology of winter intense precipitation events along the Mediterranean coasts. *Natural Hazards and Earth System Sciences*, *13*(7), 1707–1722. https://doi.org/10.5194/nhess-13-1707-2013

Robertson, A. W., Camargo, S. J., Sobel, A., Vitart, F., & Wang, S. (2018). Summary of workshop on sub-seasonal to seasonal predictability of extreme weather and climate. *npj Climate and Atmospheric Science*, *1*, 20178. https://doi.org/10.1038/s41612-017-0009-1

Sabatani, D., & Gualdi, S. (2025). ENSO teleconnections with the NAE sector during December in CMIP5/CMIP6 models: Impacts of the atmospheric mean state. *npj Climate and Atmospheric Science*, *8*(1), 226. https://doi.org/10.1038/s41612-025-01064-2

Saife, A. A., Knight, J. R., Vallis, G. K., & Folland, C. K. (2005). A stratospheric influence on the winter NAO and North Atlantic surface climate. *Geophysical Research Letters*. https://doi.org/10.1029/2005GL023226

Saji, N., Goswami, B., Vinayachandran, P., & Yamagata, T. (1999). A dipole mode in the tropical Indian Ocean. *Nature*, *401*(6751), 360–363. https://doi.org/10.1038/43854

Saji, N. H., & Yamagata, T. (2003). Possible impacts of Indian Ocean dipole mode events on global climate. *Climate Research*, *25*, 151–169. https://doi.org/10.3354/cr025151

Seager, R., Liu, H., Kushnir, Y., Osborn, T. J., Simpson, I. R., Kelley, C. R., & Nakamura, J. (2020). Mechanisms of winter precipitation variability in the European–Mediterranean region associated with the North Atlantic Oscillation. *Journal of Climate*, *33*(16), 7179–7196. https://doi.org/10.1175/jcli-d-20-0011.1

Terray, L., & Bador, M. (2025). Influence of large-scale atmospheric circulation and Mediterranean Sea surface temperature to extreme land precipitation: The case of storm Alex. *Environmental Research: Climate*, *4*(1), 015002. https://doi.org/10.1088/2752-5295/adaa0d

Ulbrich, U., Leckebusch, G. C., Grieger, J., Schuster, M., Akperov, M., Bardin, M. Y., et al. (2013). Are Greenhouse Gas Signals of Northern Hemisphere winter extra-tropical cyclone activity dependent on the identification and tracking algorithm? *Meteorologische Zeitschrift*, *22*(1), 61–68. https://doi.org/10.1127/0941-2948/2013/0420

Wang, G., Cai, W., Santoso, A., Abram, N., Ng, B., Yang, K., et al. (2024). The Indian Ocean Dipole in a warming world. *Nature Reviews Earth & Environment*, *5*(8), 588–604. https://doi.org/10.1038/s43017-024-00573-7

Weller, E., & Cai, W. (2013). Asymmetry in the IOD and ENSO teleconnection in a CMIP5 model ensemble and its relevance to regional rainfall. *Journal of Climate*, *26*(14), 5139–5149. https://doi.org/10.1175/JCLI-D-12-00789.1

White, C. J., Domeisen, D. I. V., Acharya, N., Adefisan, E. A., Anderson, M. L., Aura, S., et al. (2022). Advances in the application and utility of subseasonal-to-seasonal predictions. *Bulletin America Meteorology Social*, *103*(6), E1448–E1472. https://doi.org/10.1175/BAMS-D-20-0224.1

Yang, Y., Xie, S.-P., Wu, L., Kosaka, Y., Lau, N.-C., & Vecchi, G. A. (2015). Seasonality and predictability of the Indian Ocean dipole mode: ENSO forcing and internal variability. *Journal of Climate*, *28*(20), 8021–8036. https://doi.org/10.1175/JCLI-D-15-0078.1